Fiducial and differential Higgs cross sections
(except for Higgs transverse momentum)

Dimitris Fassouliotis
on behalf of ATLAS and CMS Collaborations

National and Kapodistrian
UNIVERSITY OF ATHENS

HIGGS2020 27/10/2020

Material in this talk

ATLAS H→ZZ→4ℓ, full 13 TeV data set, final results
Eur. Phys. J. C 80 (2020) 941
- 20 differential observables
- 8 double differential observables

ATLAS H→γγ, full 13 TeV data set, preliminary results
ATLAS-CONF-2019-029
- 6 differential observables

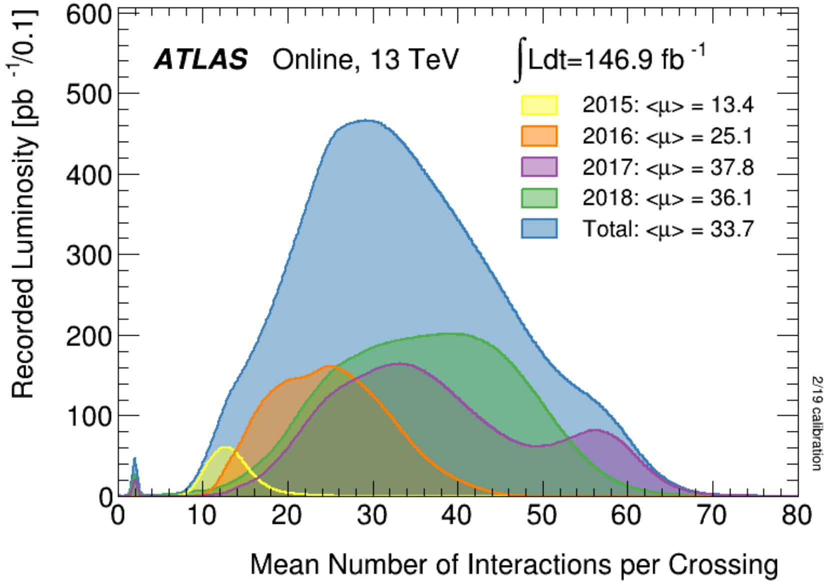

CMS H→ZZ→4ℓ, full 13 TeV data set, preliminary results
CMS-PAS-HIG-19-001
- 4 differential observables

CMS H→γγ, 2015-2016 data set
JHEP 01 (2019) 183
- 21 differential observables
- One double differential observable

CMS H→WW→eνμν, full 13 TeV data set, final results
Sub. JHEP arXiv:2007.01984
- 2 differential observables

Both experiments introduced several improvements to the reconstruction and identification of the physics objects to cope with the increased pile-up conditions in LHC Run II

Introduction – Fiducial cross sections

- LHC Run I → Discovery of the Higgs boson
- LHC Run II → Entrance to the era of precision measurements in the Higgs sector

Inclusive Higgs boson measurements are limited by systematic uncertainties

To improve the comparison of the experimental measurements with SM predictions and increase sensitivity to BSM physics →

- **Inclusive and differential fiducial cross sections measurements**

✓ Largely model independent

✓ The same measurement can be compared with many theories and models

- Restricted to compare one or two variables at a time
- Not easy to combine many channels w/o extrapolation to full phase space

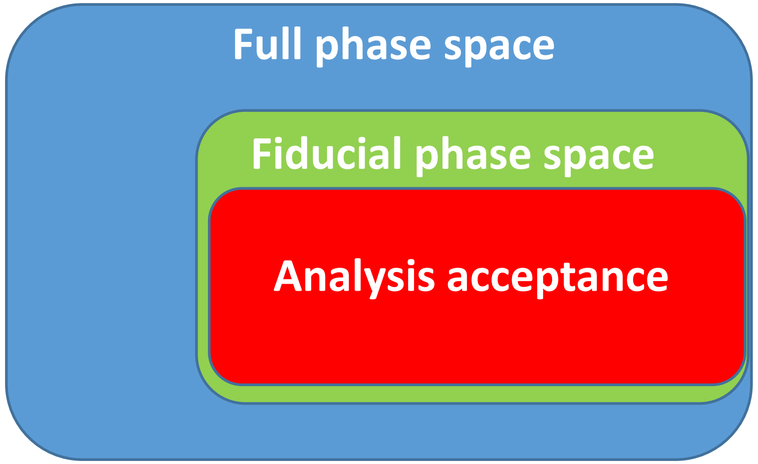

- Focus to H→ZZ, γγ and WW

Differential cross section measurements exist also for the fermionic decay channels but they address mainly Higgs p_T and have been covered in Elisa Fontanesi ‘s presentation

Example of definitions from ATLAS
Evident proximity of fiducial phase space with analysis criteria

Analysis selection

Leptons and jets	
Muons	$p_T > 5$ GeV, $\lvert\eta\rvert < 2.7$
Electrons	$E_T > 7$ GeV, $\lvert\eta\rvert < 2.47$
Jets	$p_T > 30$ GeV, $\lvert\eta\rvert < 4.5$
Lepton selection and pairing	
Lepton kinematics	$p_T > 20, 15, 10$ GeV
Leading pair (m_{12})	SFOC lepton pair with smallest $\lvert m_Z - m_{\ell\ell}\rvert$
Subleading pair (m_{34})	Remaining SFOC lepton pair with smallest $\lvert m_Z - m_{\ell\ell}\rvert$
Event selection (at most one Higgs boson candidate per channel)	
Mass requirements	50 GeV$< m_{12} <$ 106 GeV and $m_{\text{threshold}} < m_{34} <$ 115 GeV
Lepton separation:	$\Delta R(\ell_i, \ell_j) > 0.1$
Lepton/Jet separation	$\Delta R(\mu_i(e_i), \text{jet}) > 0.1(0.2)$
J/ψ veto	$m(\ell_i, \ell_j) > 5$ GeV for all SFOC lepton pairs
Impact parameter	$\lvert d_0\rvert/\sigma(d_0)$ ¡ 5 (3) for electrons (muons)
Mass window	105 GeV $< m_{4\ell} <$ 160 GeV
Vertex selection:	χ^2/N_{dof} ¡ 6 (9) for 4μ (other channels)
If extra lepton with $p_T > 12$ GeV	Quadruplet with largest matrix element (ME) value

Fiducial phase space requirements

Leptons and jets	
Leptons	$p_T > 5$ GeV, $\lvert\eta\rvert < 2.7$
Jets	$p_T > 30$ GeV, $\lvert y\rvert <$ 4.4
Lepton selection and pairing	
Lepton kinematics	$p_T > 20, 15, 10$ GeV
Leading pair (m_{12})	SFOC lepton pair with smallest $\lvert m_Z - m_{\ell\ell}\rvert$
Subleading pair (m_{34})	remaining SFOC lepton pair with smallest $\lvert m_Z - m_{\ell\ell}\rvert$
Event selection (at most one quadruplet per event)	
Mass requirements	50 GeV$< m_{12} <$ 106 GeV and 12 GeV $< m_{34} <$ 115 GeV
Lepton separation	$\Delta R(\ell_i, \ell_j) > 0.1$
Lepton/Jet separation	$\Delta R(\ell_i, \text{jet}) > 0.1$
J/ψ veto	$m(\ell_i, \ell_j) > 5$ GeV for all SFOC lepton pairs
Mass window	105 GeV $< m_{4\ell} <$ 160 GeV
If extra lepton with $p_T > 12$ GeV	Quadruplet with largest matrix element value

Similarity of the definition of the fiducial phase space to the analysis criteria can be observed in all fiducial measurements (see backup slides)

Introduction – Differential measurements

Initial distribution

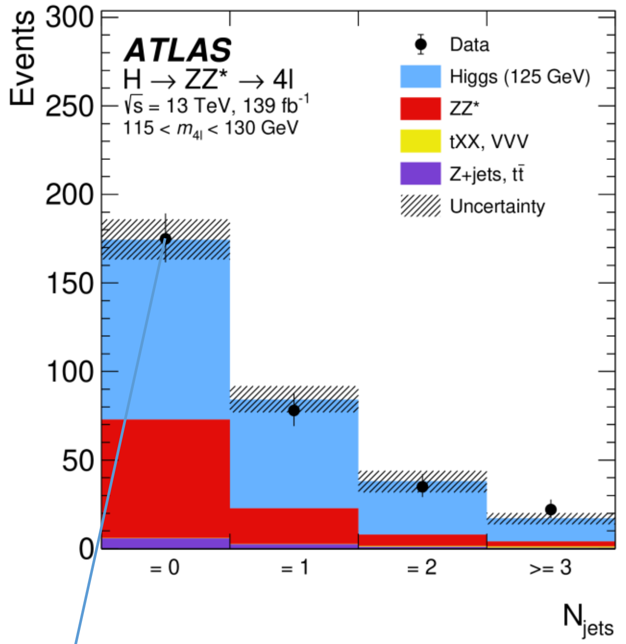

Signal Extraction and Unfolding

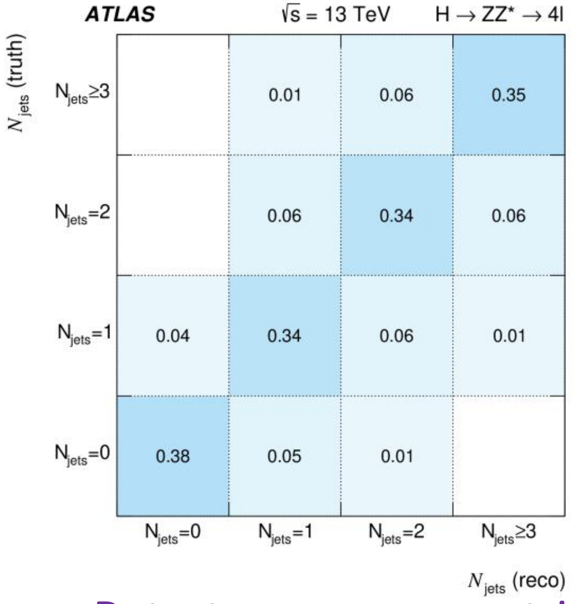

Detector response matrix

Fiducial differential cross section

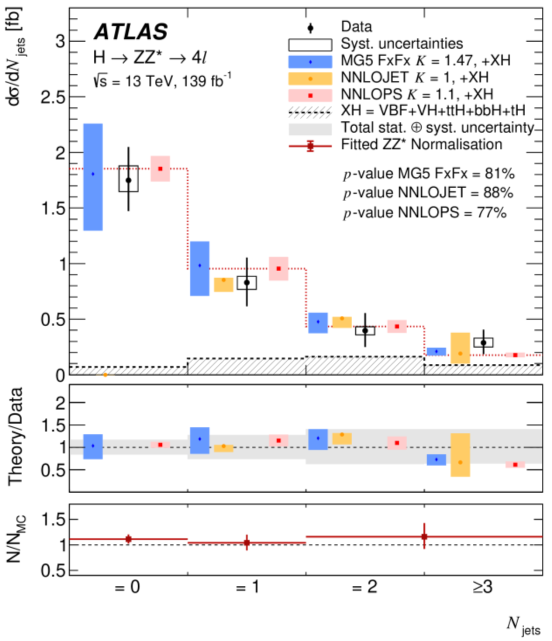

$$N_i(m_{4\ell}) = \sum_j r_{ij} \cdot (1 + f_i^{\mathrm{nonfid}}) \cdot \sigma_j^{\mathrm{fid}} \cdot \mathcal{P}_i(m_{4\ell}) \cdot \mathcal{L} + N_i^{\mathrm{bkg}}(m_{4\ell})$$

Signal shape from MC

$$\sigma_j^{\mathrm{fid}} = \sigma_j \cdot A_j \cdot \mathcal{B}$$

Interpretation
Comparison with theoretical models

H→ZZ→4ℓ - Inclusive fiducial xs

Fully reconstructed final state BR ~ 0.0124% - S/B ~ 2

- **4 low-pT isolated leptons (electrons / muons), originating from the PV**
- Main background: ZZ continuum, shape from MC & normalization from data sideband (ATLAS)
- Data driven estimated reducible backgrounds
- Fit on m4l (simultaneous fit on all decay final states for the differential distributions)

EPJC arXiv:2004.03969

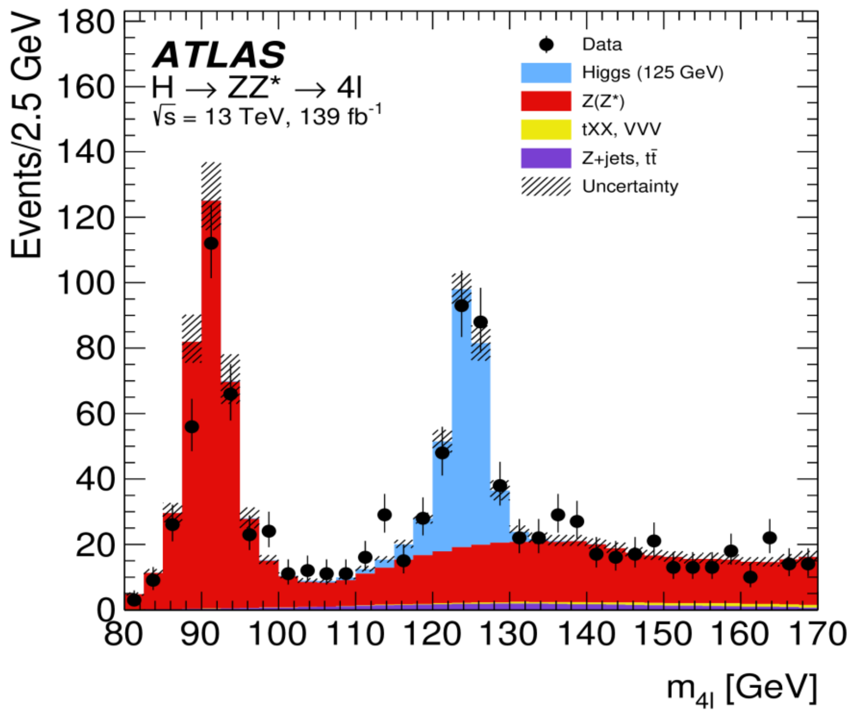

CMS-PAS-HIG-19-001

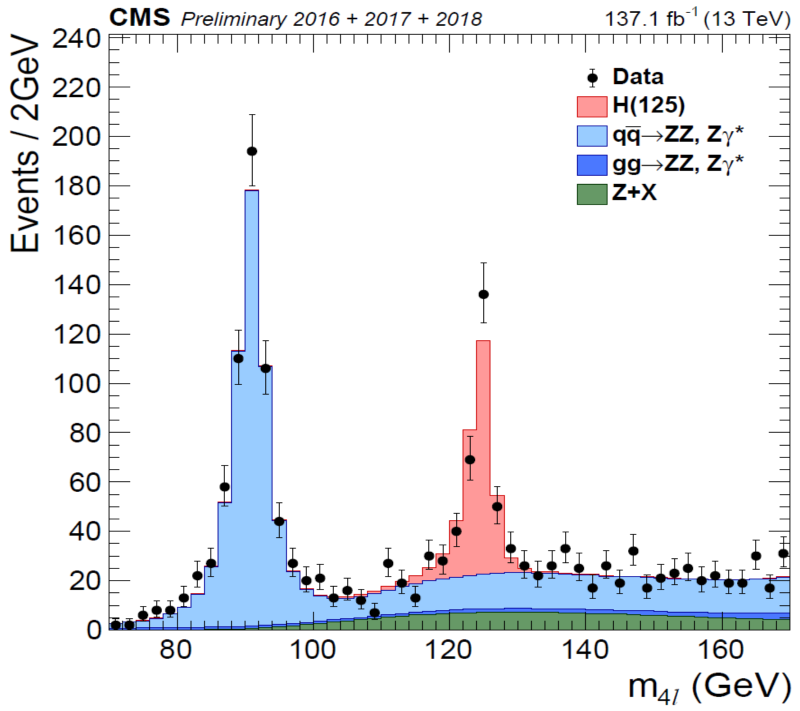

H→ZZ→4ℓ - fiducial xs in different decay channels

EPJC arXiv:2004.03969

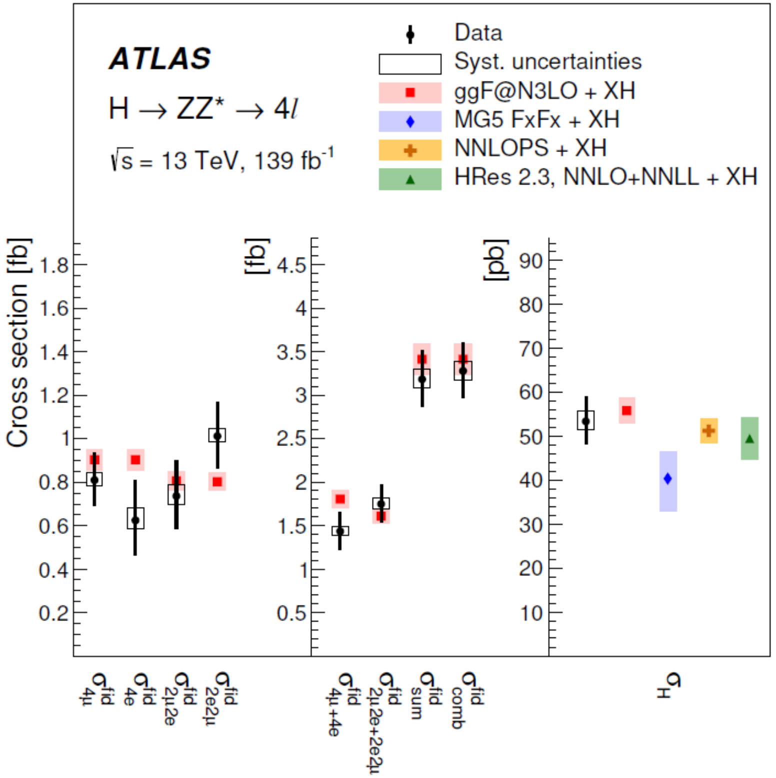

CMS-PAS-HIG-19-001

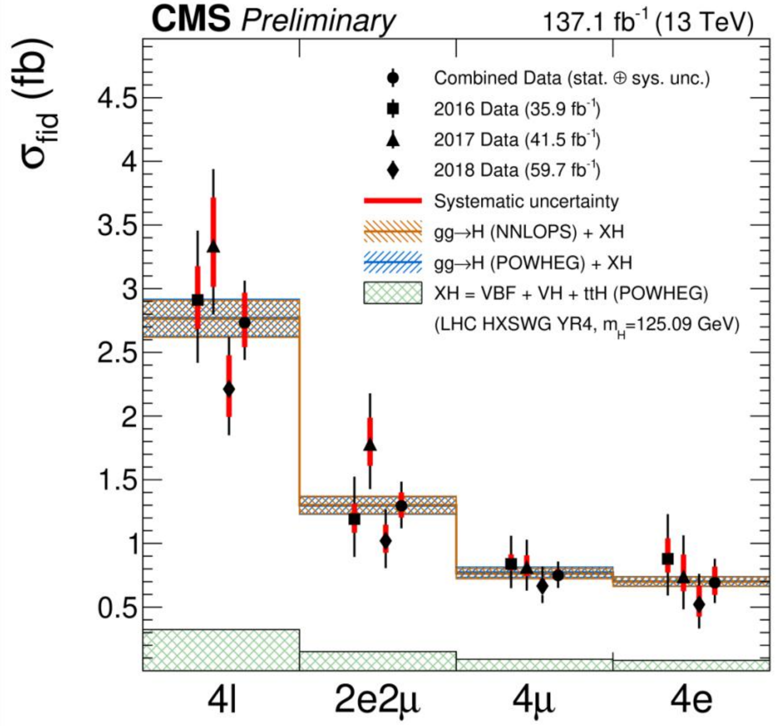

Compatible with SM

Main differences

ATLAS		CMS
$\|\eta\|<2.7$	-	$\|\eta\|<2.5$
$p^{\ell}_{T}>5$ GeV	-	$p^{e}_{T}>7$ GeV
		$p^{\mu}_{T}>5$ GeV

$$\sigma_{fid} = 3.28 \pm 0.30(stat) \pm 0.11(syst)\ fb$$ (SM relative BRs assumed)

$$\sigma_{fid} = 3.18 \pm 0.31(stat) \pm 0.11(syst)\ fb$$

$$\sigma_{fid,SM} = 3.41 \pm 0.18\ fb$$

$$\sigma_{fid} = 2.73^{+0.23}_{-0.22}(stat)^{+0.24}_{-0.19}(syst)\ fb$$

$$\sigma_{fid,SM} = 2.76 \pm 0.14\ fb$$

(Simultaneous fit with BRs allowed to flow)

H→γγ - Inclusive fiducial xs

Fully reconstructed final state

BR ~ 0.2% - S/B <0.1

- **Two isolated photons**
- Background: γγ continuum, γ j and j j estimated from data sideband

- Multivariate methods to estimate the γγ vertex
- Subcategories according to di-photon mass resolution (CMS)
- Estimation of fraction of each background component for each cross section bin using sidebands (ATLAS)
- Fit to $m_{\gamma\gamma}$ spectrum

Main differences

ATLAS |η|<2.37 excl. 1.37<|η|<1.52

CMS |η|<2.5

ATLAS-CONF-2019-029

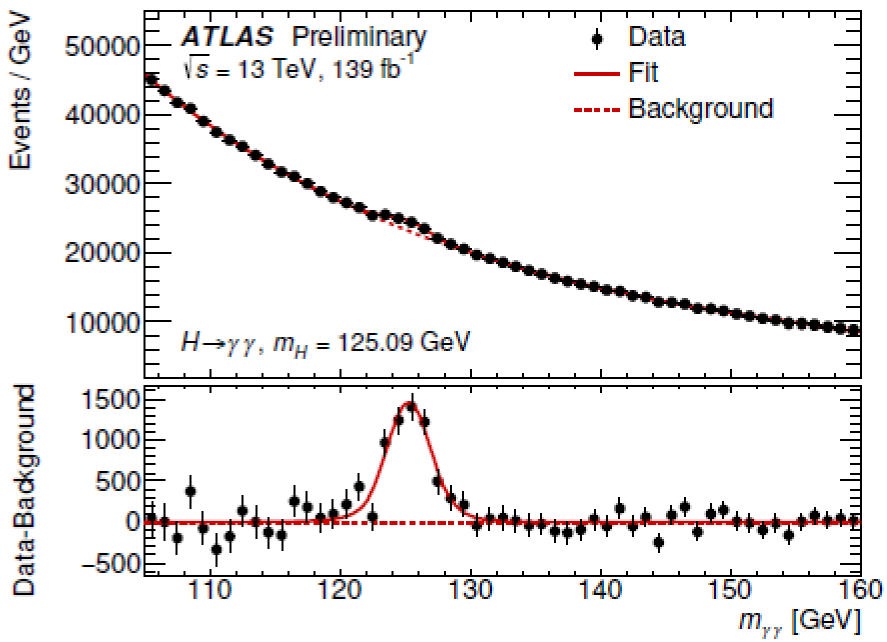

$$\sigma_{fid} = 65.2 \pm 4.5(stat) \pm 5.6(syst)\ fb$$

$$\sigma_{fid,SM} = 63.6 \pm 3.3\ fb$$

Compatible with SM

JHEP 01 (2019) 183

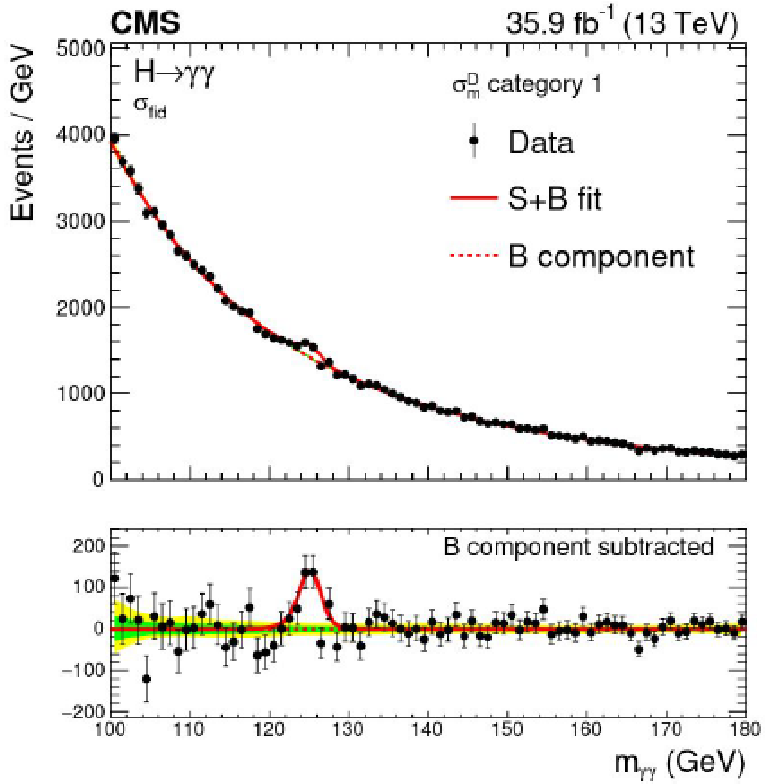

$$\sigma_{fid} = 84 \pm 11(stat) \pm 7(syst)\ fb$$

$$\sigma_{fid,SM} = 73 \pm 4\ fb$$

H→ZZ→4ℓ, H→γγ : y_H

- Sensitive to BSM effects
- Sensitive to pQCD Higgs production modeling and PDFs

Statistical uncertainty dominant both for 4ℓ and γγ

Some difference between data and expectations can be observed … but not really significant

Negligible correlation between signal bins

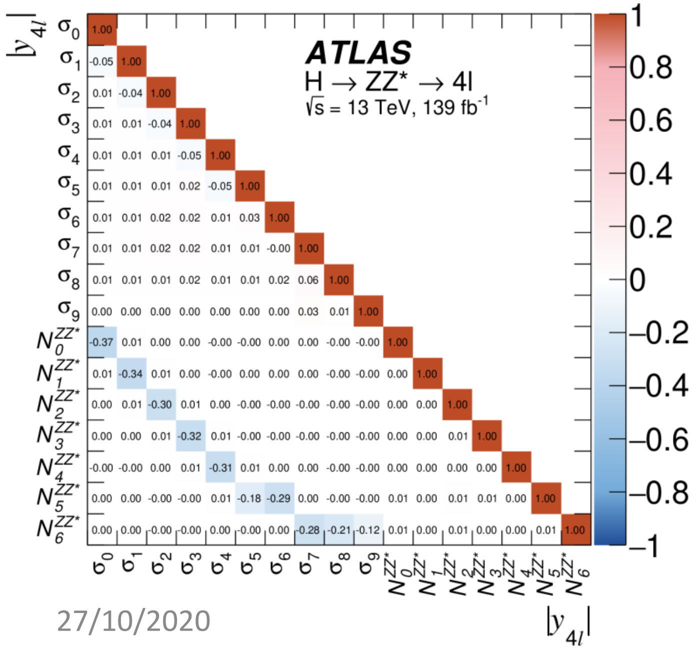

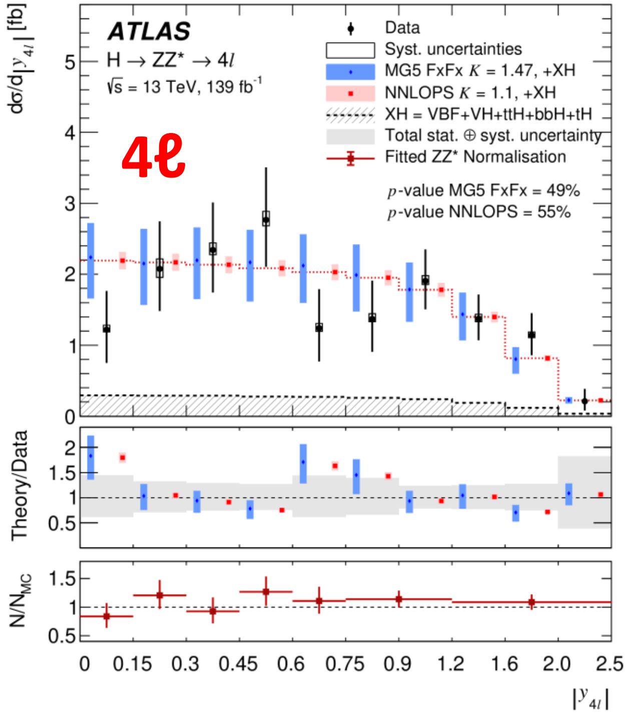

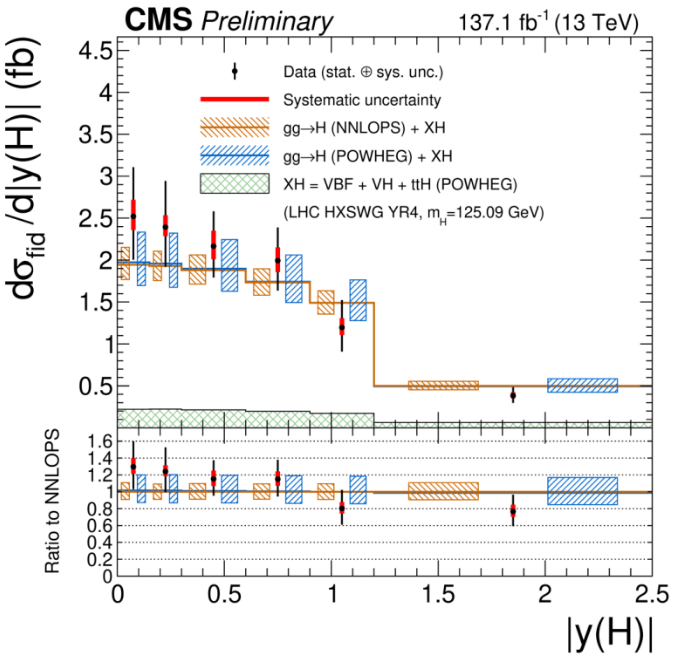

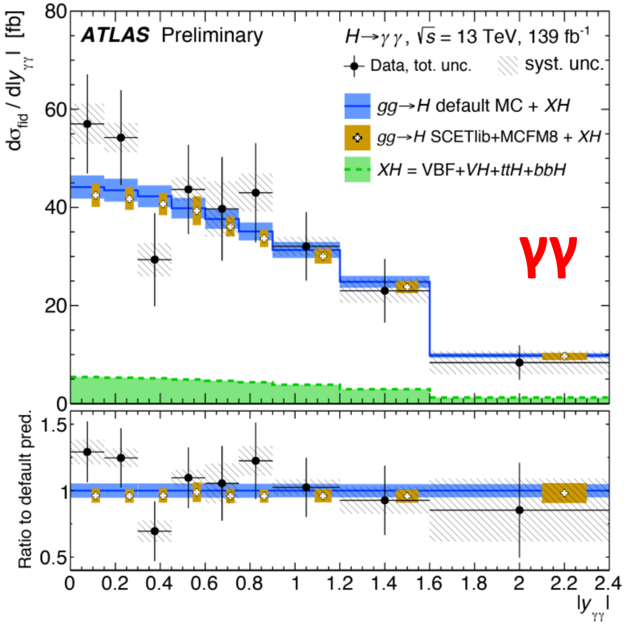

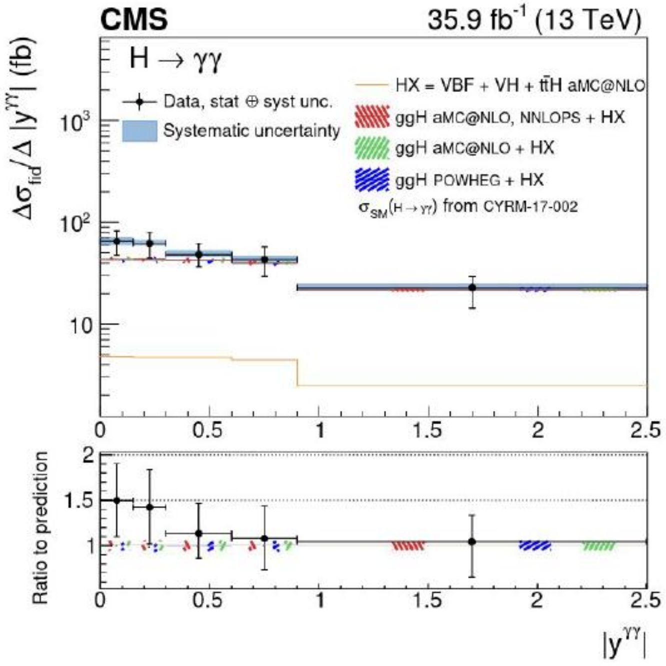

H→ZZ→4ℓ : N jets

- Probe relative contribution from different Higgs production mechanisms
- Sensitive to pQCD radiation

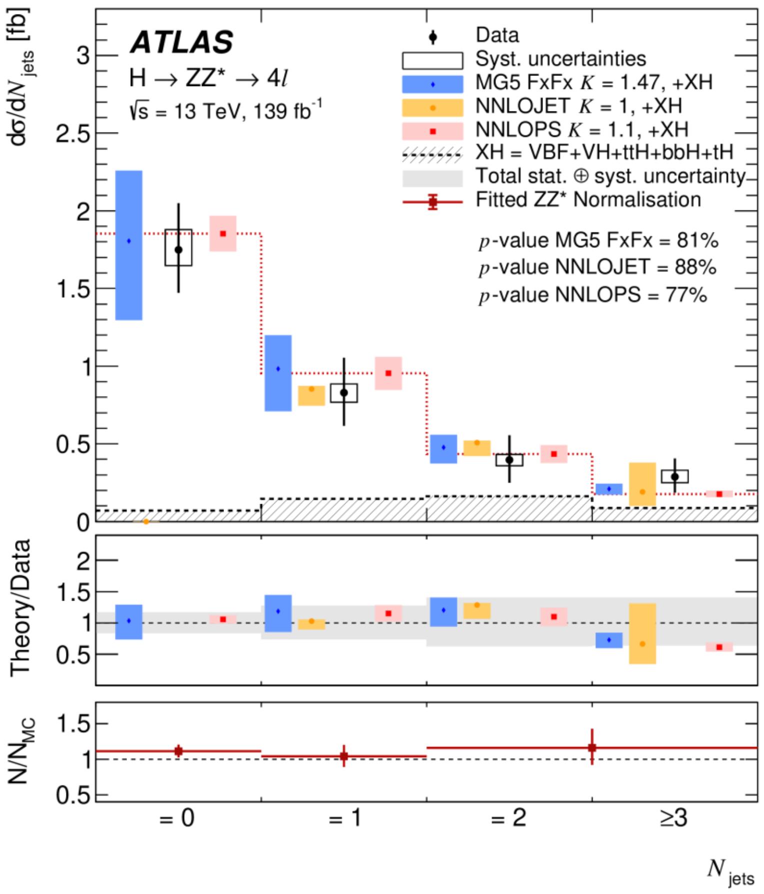

Correlation matrix

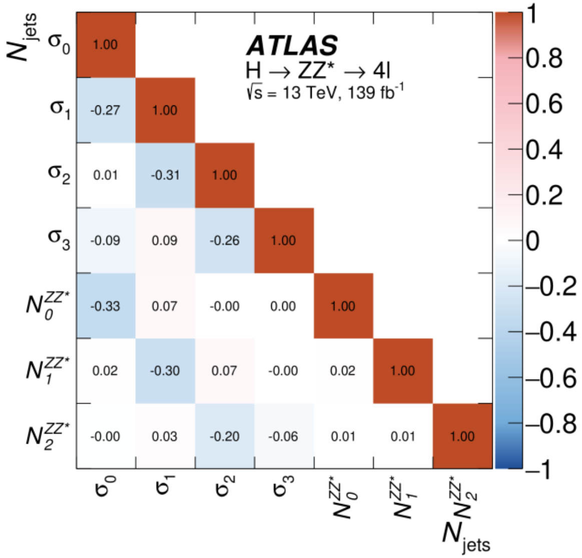

	σ0	σ1	σ2	σ3	$N_0^{ZZ^*}$	$N_1^{ZZ^*}$	$N_2^{ZZ^*}$
σ0	1.00						
σ1	-0.27	1.00					
σ2	0.01	-0.31	1.00				
σ3	-0.09	0.09	-0.26	1.00			
$N_0^{ZZ^*}$	-0.33	0.07	-0.00	0.00	1.00		
$N_1^{ZZ^*}$	0.02	-0.30	0.07	-0.00	0.02	1.00	
$N_2^{ZZ^*}$	-0.00	0.03	-0.20	-0.06	0.01	0.01	1.00

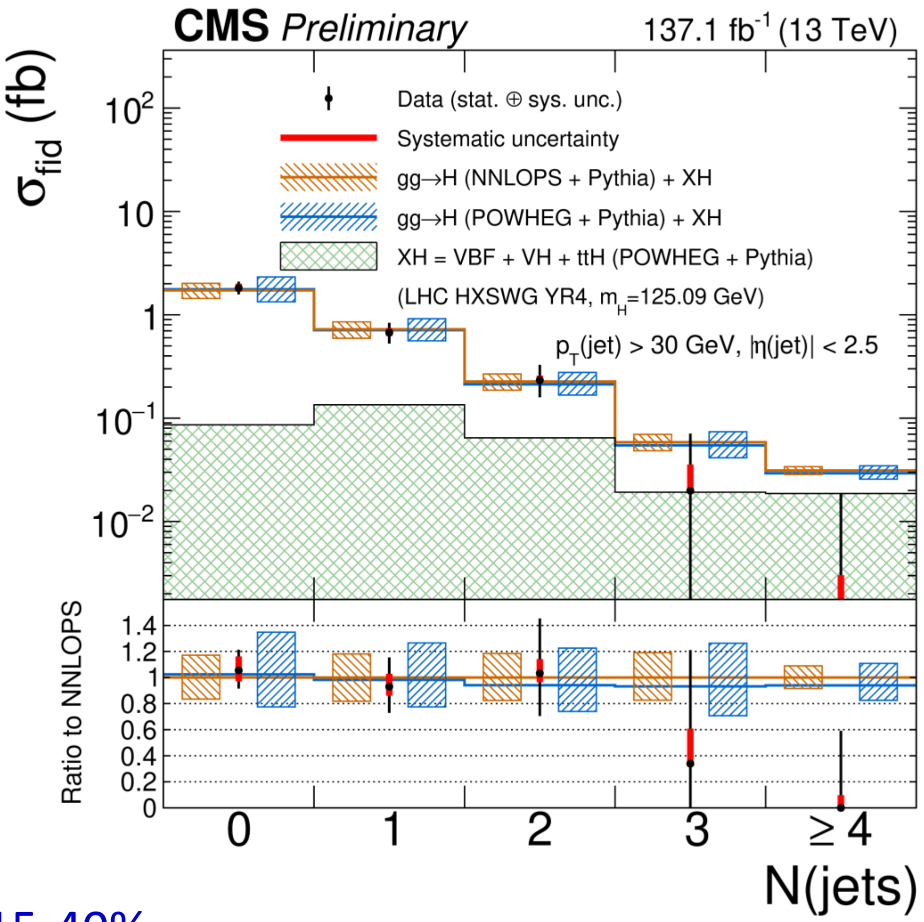

Statistical uncertainty dominant 15-40%

Compatible with predictions

H→γγ : N jets

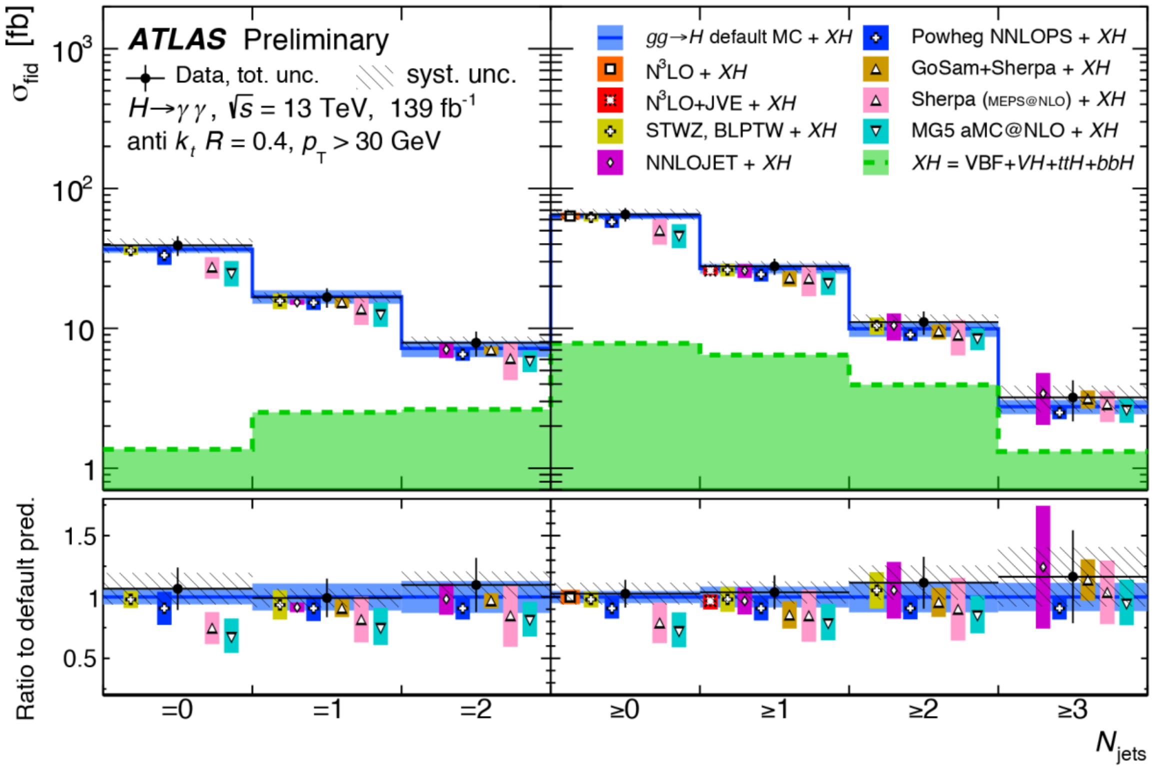

Compatible with predictions

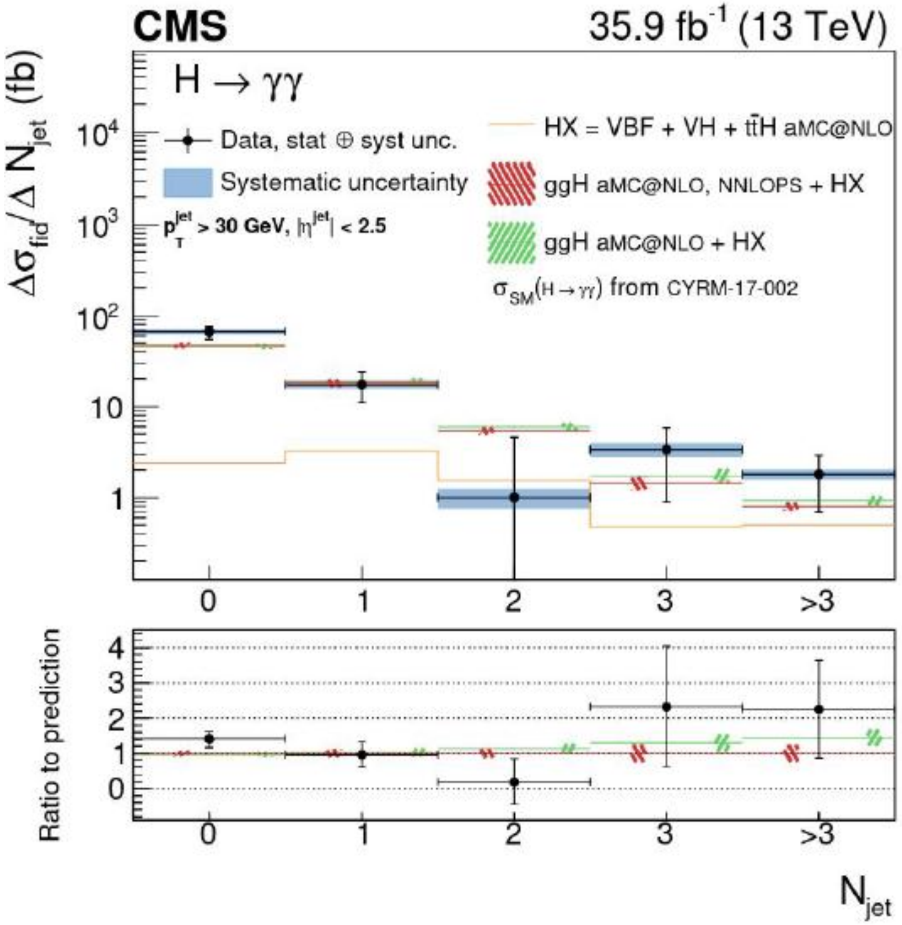

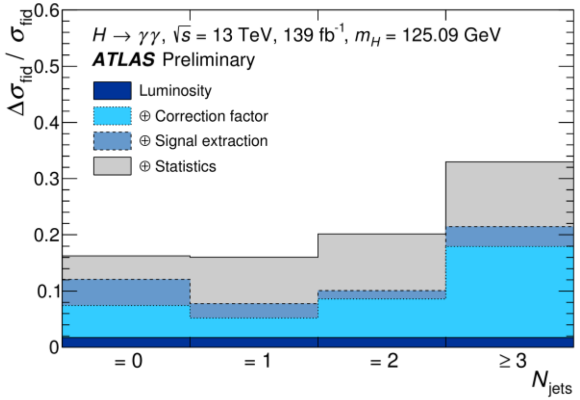

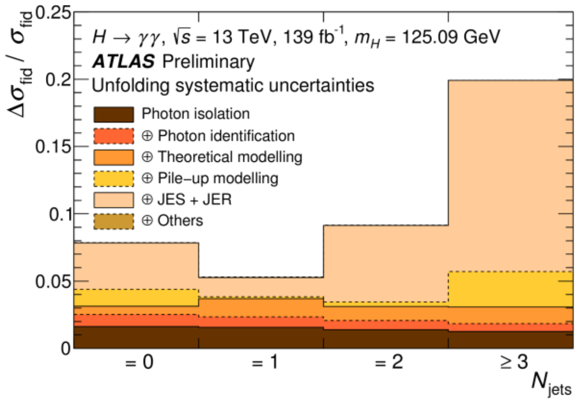

Break down of uncertainties

H→WW→eνμν : N jets

Not fully reconstructed final state but large BR

Fully leptonic final state with different flavor leptons

Backgrounds WW, top quark, non prompt leptons

- 2D template fit of m_{ll} and m_T
- Subcategories according to lepton flavor and p^H_T

JHEP arXiv:2007.01984

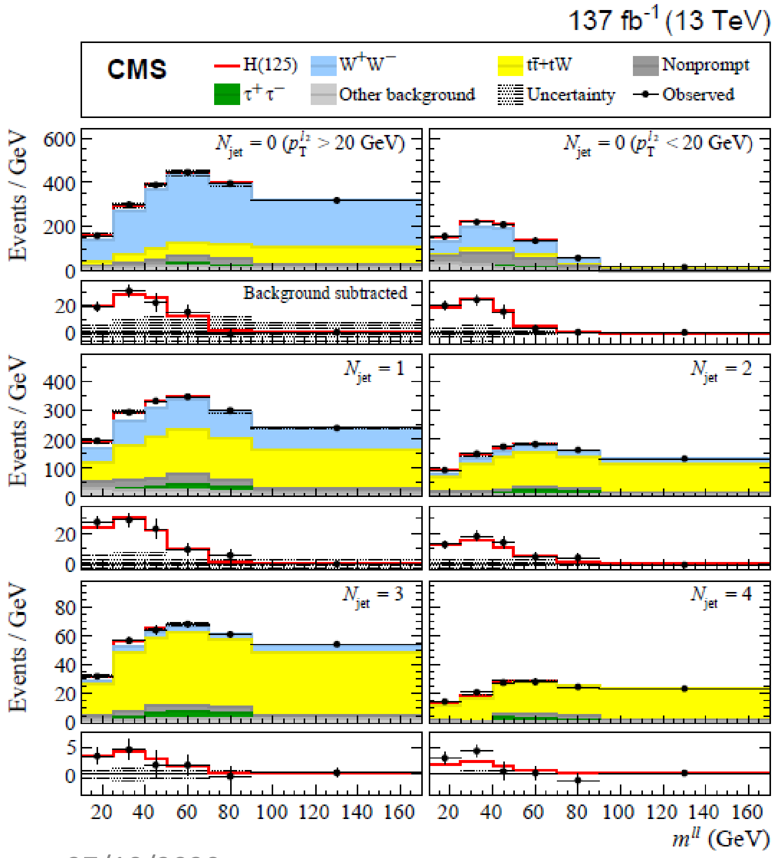

Compatible with SM

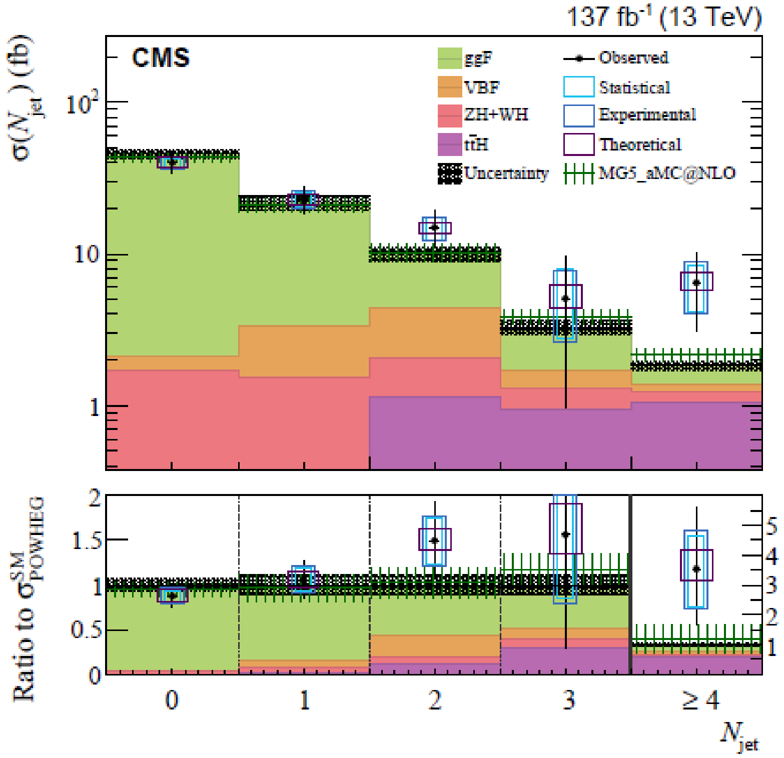

$$\sigma_{fid} = 86.5 \pm 4.1(stat) \pm 8.6(syst)\ fb$$

$$\sigma_{fid,SM} = 82.5 \pm 4.2\ fb$$

H→ZZ→4ℓ, H→γγ : p^j_T

- ➢ Probe relative contribution from different Higgs production mechanisms
- ➢ Sensitive to pQCD radiation

Statistical uncertainty dominant

Compatible with predictions

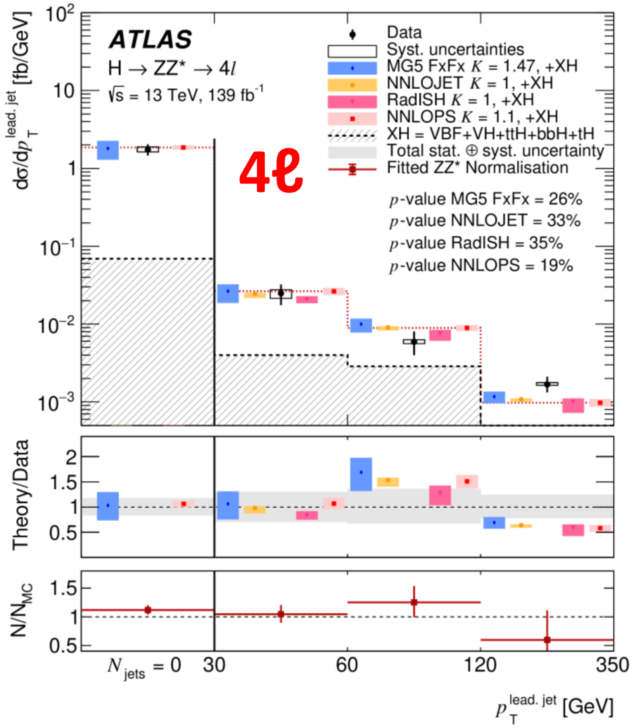

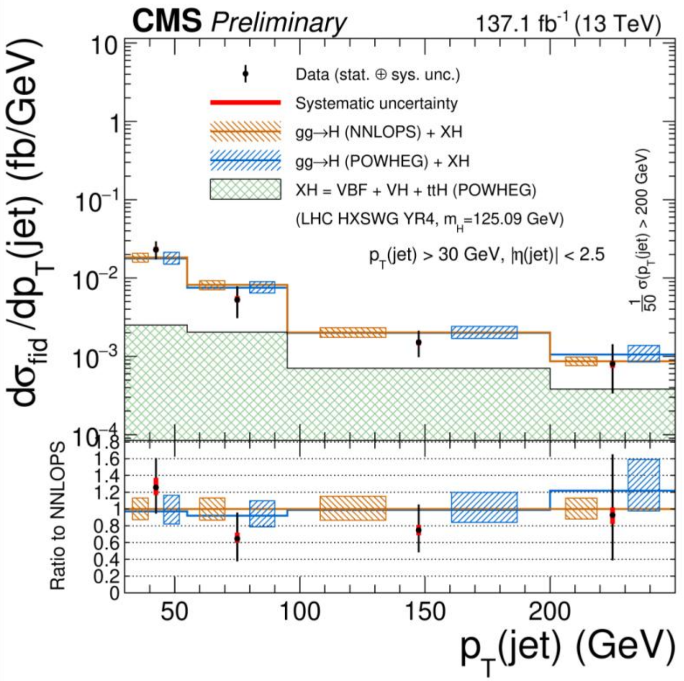

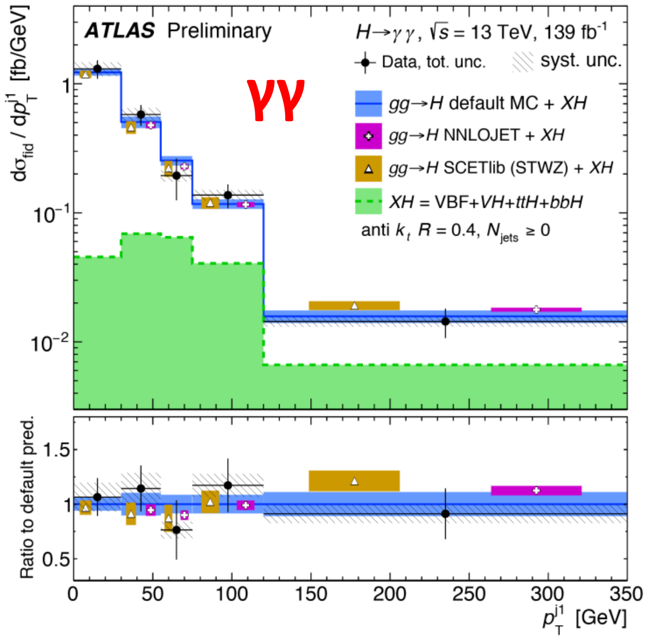

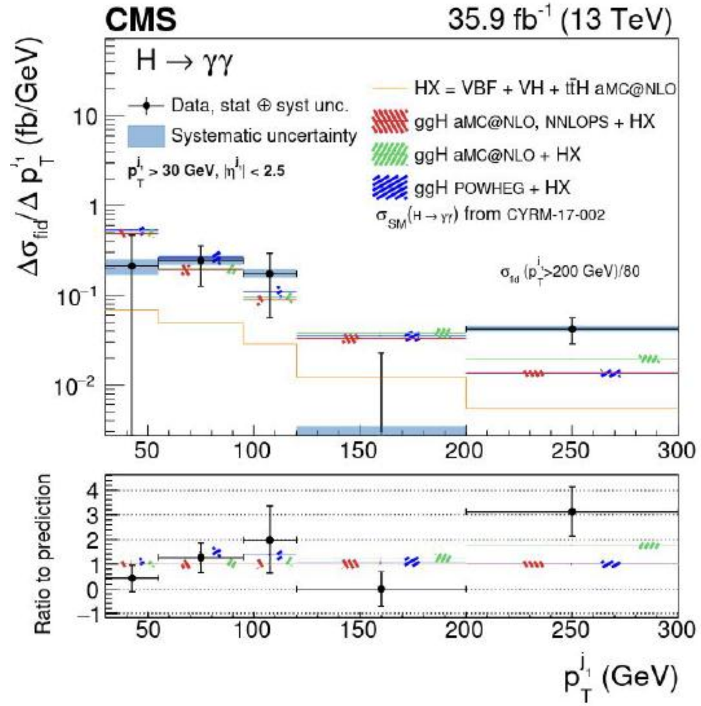

H→ZZ→4ℓ : $m_{12(Z1)}$ vs $m_{34(Z2)}$

1d distributions

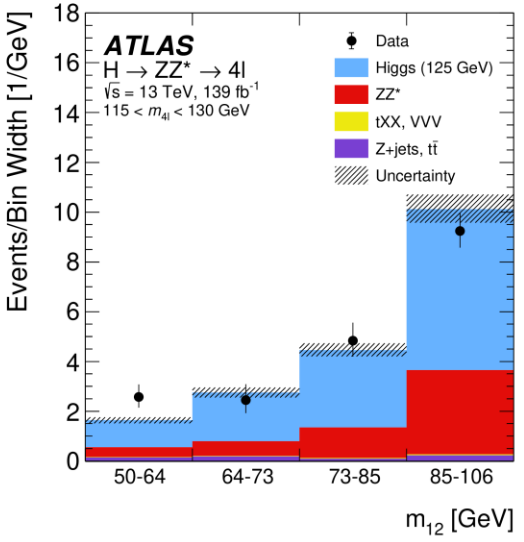

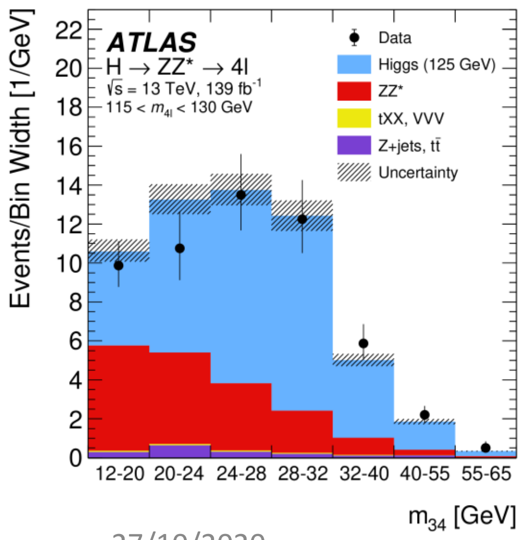

2d pre-fit distribution

binning such that stat. unc. ≤ 20%

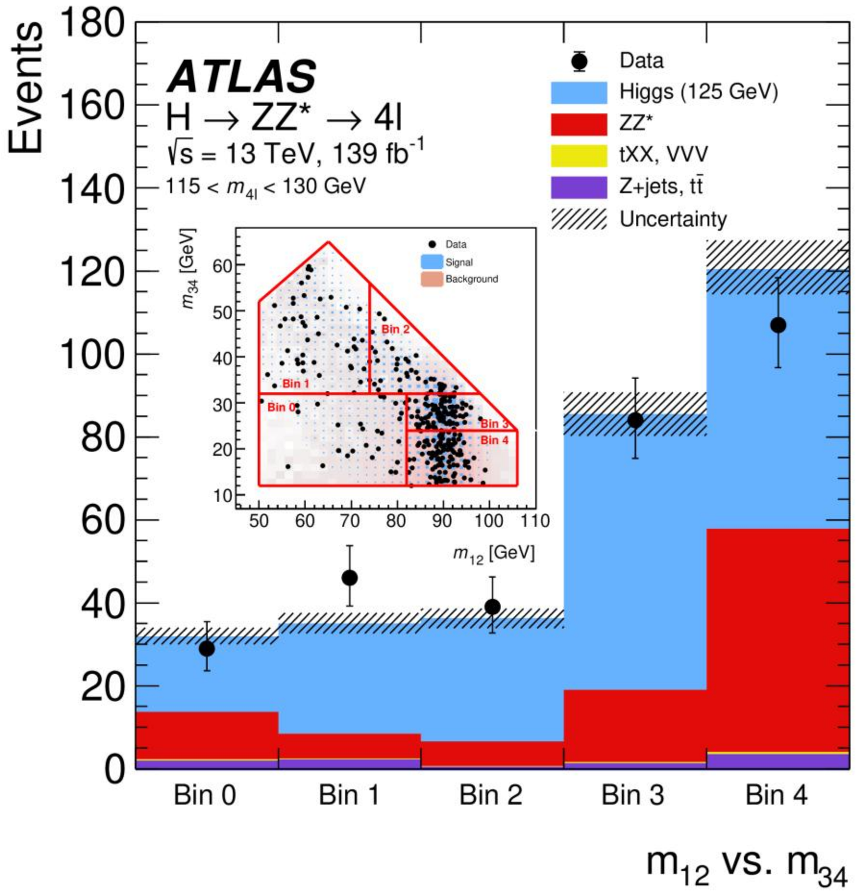

Det. response matrix

Very small migration between bins

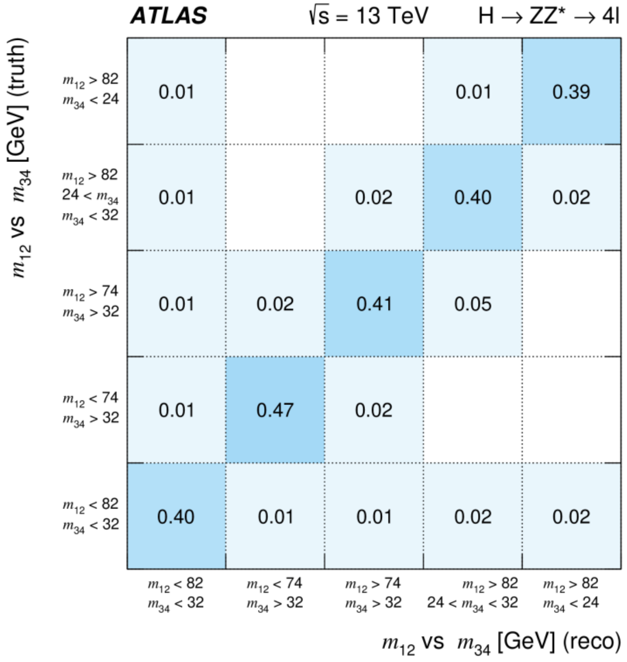

H→ZZ→4ℓ : $m_{12(Z1)}$ vs $m_{34(Z2)}$

Differential fiducial cross section

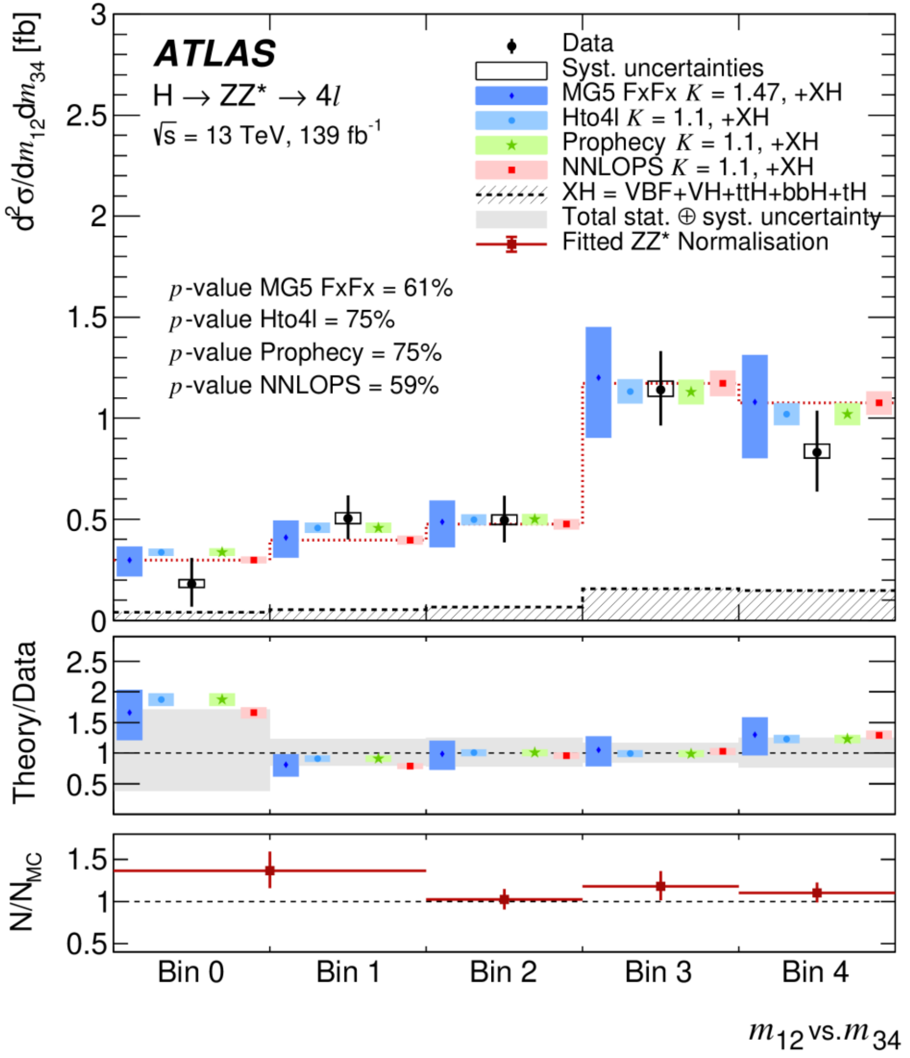

Compatible with predictions

Interpretation in terms of pseudo-observables to constrain BSM contact terms

Pseudo-observables affecting the angular distributions are set to zero

Flavor universal contact terms

Contact terms are assumed equal for e and μ, but can be different for left- and right- handed leptons

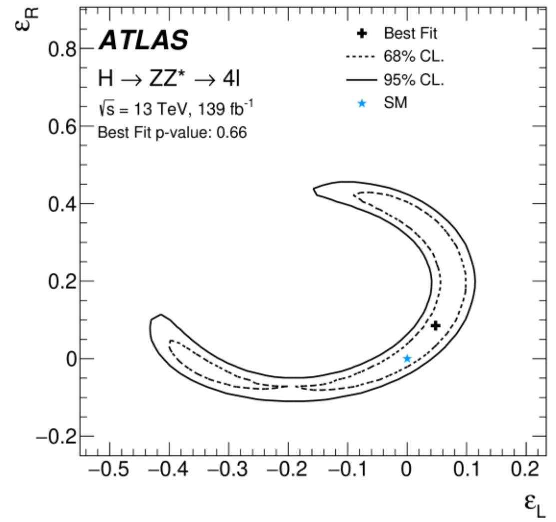

Flavor non universal vector contact terms

Lepton-flavour universality is not assumed. The helicity structure of the BSM couplings is fixed to be vector

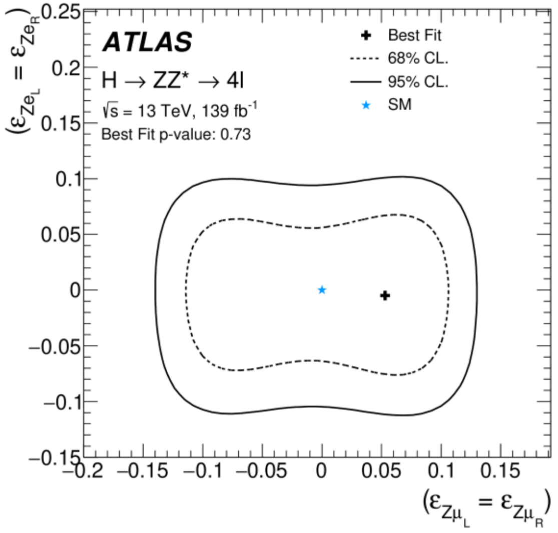

Summary

- With the run II of LHC, Higgs physics entered the era of precision measurements
- Both ATLAS and CMS improved a lot their analyses to cope with the high pile-up conditions
- To be as model independent as possible a lot of fiducial measurements have been performed by ATLAS and CMS both inclusive and differential, which can easily be compared to theoretical models
- Up to now, despite small differences, **theoretical expectations are shown to be compatible with the data**
- Part of the inclusive and most of the differential measurements are dominated by statistical uncertainties, thus results from the run III of LHC are anticipated anxiously

Thank you
for your attention

Back up slides

H→ZZ→4ℓ

Fiducial phase space definition in CMS

Requirements for the H $\rightarrow 4\ell$ fiducial phase space	
Lepton kinematics and isolation	
Leading lepton p_T	$p_T > 20$ GeV
Next-to-leading lepton p_T	$p_T > 10$ GeV
Additional electrons (muons) p_T	$p_T > 7(5)$ GeV
Pseudorapidity of electrons (muons)	$\|\eta\| < 2.5(2.4)$
Sum of scalar p_T of all stable particles within $\Delta R < 0.3$ from lepton	$< 0.35 \cdot p_T$
Event topology	
Existence of at least two same-flavor OS lepton pairs, where leptons satisfy criteria above	
Inv. mass of the Z_1 candidate	$40\,\mathrm{GeV} < m_{Z_1} < 120\,\mathrm{GeV}$
Inv. mass of the Z_2 candidate	$12\,\mathrm{GeV} < m_{Z_2} < 120\,\mathrm{GeV}$
Distance between selected four leptons	$\Delta R(\ell_i, \ell_j) > 0.02$ for any $i \neq j$
Inv. mass of any opposite sign lepton pair	$m_{\ell^+\ell'^-} > 4\,\mathrm{GeV}$
Inv. mass of the selected four leptons	$105\,\mathrm{GeV} < m_{4\ell} < 140\,\mathrm{GeV}$

$H \rightarrow \gamma\gamma$

Fiducial phase space definition in ATLAS

Objects	Fiducial definition
Photons	$\|\eta\|<2.37$ (excluding $1.37<\|\eta\|<1.52$), $\Sigma p^{i}_{T}/p^{\gamma}_{T} <0.05$
Jets	anti-kt, R=0.4. $p_T>30$ GeV, $\|y\|<4.4$
Diphoton	$N_\gamma \geq 2$, 105 GeV < $m_{\gamma\gamma}$ < 160 GeV, $p^{\gamma 1}_{T}/m_{\gamma\gamma} > 0.35$, $p^{\gamma 2}_{T}/m_{\gamma\gamma} > 0.25$

Fiducial phase space definition in CMS

Objects	Fiducial definition
Photons	$\|\eta\|<2.5$, $\Sigma p^{i}_{T} <10$ GeV
Jets	anti-kt, R=0.4. $p_T>30$ GeV, $\|y\|< 2.5$ (4.7)
Diphoton	$N_\gamma \geq 2$, 100 GeV < $m_{\gamma\gamma}$ < 180 GeV, $p^{\gamma 1}_{T}/m_{\gamma\gamma} > 1/3$, $p^{\gamma 2}_{T}/m_{\gamma\gamma} > 1/4$

H→ZZ→4ℓ

Fiducial cross section measurements in ATLAS
In specific decay final states and inclusive

Cross section [fb]	Data (± (stat.) ± (syst.))			Standard Model prediction		p-value [%]
$\sigma_{4\mu}$	0.81	±0.12	±0.03	0.90	± 0.05	46
σ_{4e}	0.62	±0.17	±0.05	0.90	± 0.05	14
$\sigma_{2\mu 2e}$	0.74	±0.15	±0.05	0.80	± 0.04	67
$\sigma_{2e2\mu}$	1.01	±0.15	±0.03	0.80	± 0.04	15
$\sigma_{4\mu+4e}$	1.43	±0.21	±0.05	1.81	± 0.10	10
$\sigma_{2\mu 2e+2e2\mu}$	1.75	±0.21	±0.06	1.61	± 0.09	51
σ_{sum}	3.18	±0.31	±0.11	3.41	± 0.18	49
σ_{comb}	3.28	±0.30	±0.11	3.41	± 0.18	67
σ_{tot} [pb]	53.5	±4.9	±2.1	55.7	± 2.8	66

H→WW→eνμν

Fiducial phase space definition in CMS

Observable	Condition
Lepton origin	Direct decay of $H \to W^+W^-$
Lepton flavors; lepton charge	e μ (not from τ decay); opposite
Leading lepton p_T	$p_T^{l_1} > 25\,GeV$
Trailing lepton p_T	$p_T^{l_2} > 13\,GeV$
$\|\eta\|$ of leptons	$\|\eta\| < 2.5$
Dilepton mass	$m^{ll} > 12\,GeV$
p_T of the dilepton system	$p_T^{ll} > 30\,GeV$
Transverse mass using trailing lepton	$m_T^{l_2} > 30\,GeV$
Higgs boson transverse mass	$m_T^H > 60\,GeV$

Observed signal strength modifiers, uncertainties and cross sections in fiducial Njet bins

N_{jet}	σ^{SM} (fb)	μ Value	stat	exp	signal	bkg	lumi	σ^{obs} (fb)
0	45.70	0.88 ± 0.13	±0.06	±0.08	±0.01	±0.07	±0.03	40.1 ± 6.0
1	21.74	1.06 ± 0.20	±0.12	±0.14	±0.01	±0.08	±0.03	23.0 ± 4.6
2	9.99	1.50 ± 0.40	$^{+0.25}_{-0.28}$	±0.28	±0.04	±0.11	±0.03	15.0 ± 4.2
3	3.26	$1.56^{+1.35}_{-1.26}$	$^{+0.89}_{-0.71}$	$^{+0.84}_{-0.76}$	$^{+0.17}_{-0.07}$	$^{+0.29}_{-0.19}$	$^{+0.07}_{-0.04}$	$5.1^{+4.4}_{-4.1}$
≥ 4	1.83	$3.54^{+2.05}_{-1.86}$	$^{+1.10}_{-1.28}$	$^{+1.28}_{-1.32}$	$^{+0.40}_{-0.20}$	$^{+0.38}_{-0.34}$	$^{+0.10}_{-0.07}$	$6.5^{+3.8}_{-3.4}$

H→ZZ→4ℓ

Definitions of observables for which differential cross sections are measured in **ATLAS**

Higgs boson kinematic-related variables	
$p_T^{4\ell}$, $\|y_{4\ell}\|$	Transverse momentum and rapidity of the four-lepton system
m_{12}, m_{34}	Invariant mass of the leading and subleading lepton pair
$\|\cos\theta^*\|$	Magnitude of the cosine of the decay angle of the leading lepton pair in the four-lepton rest frame relative to the beam axis
$\cos\theta_1$, $\cos\theta_2$	Production angles of the anti-leptons from the two Z bosons, where the angle is relative to the Z vector.
ϕ, ϕ_1	Two azimuthal angles between the three planes constructed from the Z bosons and leptons in the Higgs boson rest frame.
Jet-related variables	
N_{jets}, $N_{b\text{-jets}}$	Jet and b-jet multiplicity
$p_T^{\text{lead. jet}}$, $p_T^{\text{sublead. jet}}$	Transverse momentum of the leading and subleading jet, for events with at least one and two jets, respectively. Here, the leading jet refers to the jet with the highest p_T in the event, while subleading refers to the jet with the second-highest p_T.
m_{jj}, $\|\Delta\eta_{jj}\|$, $\Delta\phi_{jj}$	Invariant mass, difference in pseudorapidity, and signed difference in ϕ of the leading and subleading jets for events with at least two jets
Higgs boson and jet-related variables	
$p_T^{4\ell j}$, $m_{4\ell j}$	Transverse momentum and invariant mass of the four-lepton system and leading jet, for events with at least one jet
$p_T^{4\ell jj}$, $m_{4\ell jj}$	Transverse momentum and invariant mass of the four-lepton system and leading and subleading jets, for events with at least two jets

H→γγ

Definition of the binning for the fiducial differential cross sections measured in **CMS**

Phase space	Observable	Bin boundaries							
Baseline $p_T^{\gamma_1}/m_{\gamma\gamma} > 1/3$ $p_T^{\gamma_2}/m_{\gamma\gamma} > 1/4$ $\|\eta^\gamma\| < 2.5$ $\text{Iso}_{\text{gen}}^{\gamma} < 10\,\text{GeV}$	$p_T^{\gamma\gamma}$ (GeV)	0	15	30	45	80	120	200	350	∞
	N_{jet}	0	1	2	3	4	∞			
	$\|y^{\gamma\gamma}\|$	0	0.15	0.3	0.6	0.9	2.5			
	$\|\cos(\theta^*)\|$	0	0.1	0.25	0.35	0.55	1			
	$p_T^{\gamma\gamma}$ (GeV), $N_{\text{jet}} = 0$	0	20	60	∞					
	$p_T^{\gamma\gamma}$ (GeV), $N_{\text{jet}} = 1$	0	60	120	∞					
	$p_T^{\gamma\gamma}$ (GeV), $N_{\text{jet}} > 1$	0	150	300	∞					
	$N_{\text{jet}}^{\text{b}}$	0	1	2	∞					
	N_{lepton}	0	1	2	∞					
	p_T^{miss} (GeV)	0	100	200	∞					
1-jet Baseline + $\geq$1 jet $p_T^j > 30\,\text{GeV}$, $\|\eta^j\| < 2.5$	$p_T^{j_1}$ (GeV)	0	45	70	110	200	∞			
	$\|y^{j_1}\|$	0	0.5	1.2	2	2.5				
	$\|\Delta\phi^{\gamma\gamma,j_1}\|$	0	2.6	2.9	3.03	π				
	$\|\Delta y^{\gamma\gamma,j_1}\|$	0	0.6	1.2	1.9	∞				
2-jets Baseline + $\geq$2 jets $p_T^j > 30\,\text{GeV}$, $\|\eta^j\| < 4.7$	$p_T^{j_2}$ (GeV)	0	45	90	∞					
	$\|y^{j_2}\|$	0	1.2	2.5	4.7					
	$\|\Delta\phi^{j_1,j_2}\|$	0	0.9	1.8	π					
	$\|\Delta\phi^{\gamma\gamma,j_1 j_2}\|$	0	2.9	3.05	π					
	$\|\bar{\eta}_{j_1 j_2} - \eta_{\gamma\gamma}\|$	0	0.5	1.2	∞					
	$m^{j_1 j_2}$ (GeV)	0	100	150	450	1000	∞			
	$\|\Delta\eta^{j_1,j_2}\|$	0	1.6	4.3	∞					
VBF-enriched 2-jets + $\|\Delta\eta^{j_1,j_2}\| > 3.5$, $m^{j_1 j_2} > 200\,\text{GeV}$	$p_T^{j_2}$ (GeV)	0	45	90	∞					
	$\|\Delta\phi^{j_1,j_2}\|$	0	0.9	1.8	π					
	$\|\Delta\phi^{\gamma\gamma,j_1 j_2}\|$	0	2.9	3.05	π					

H→γγ

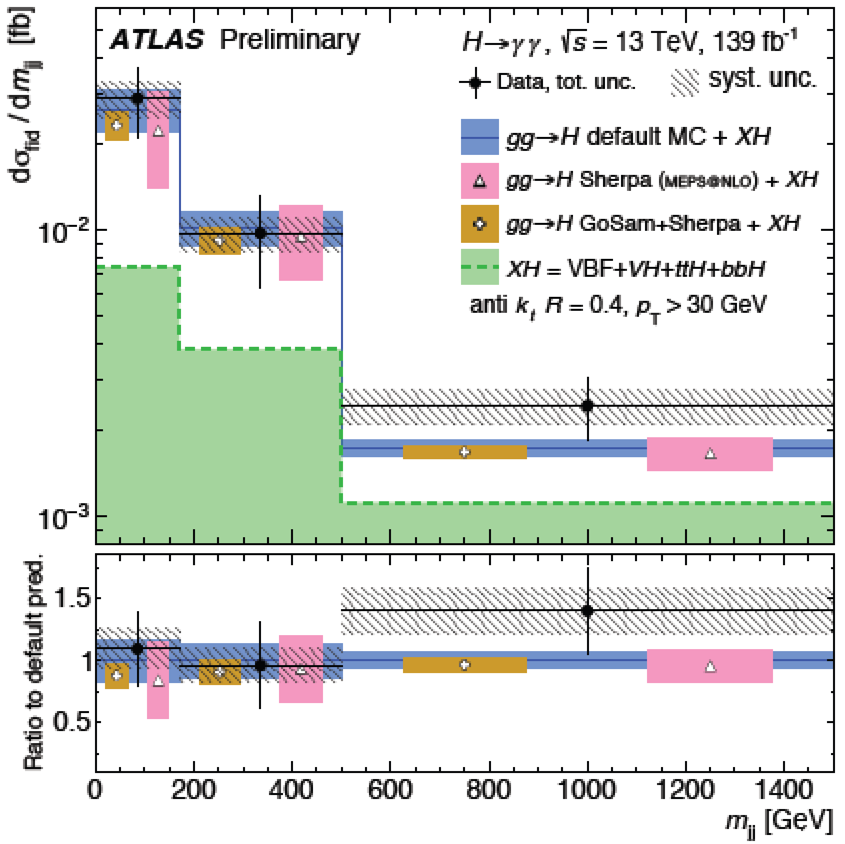

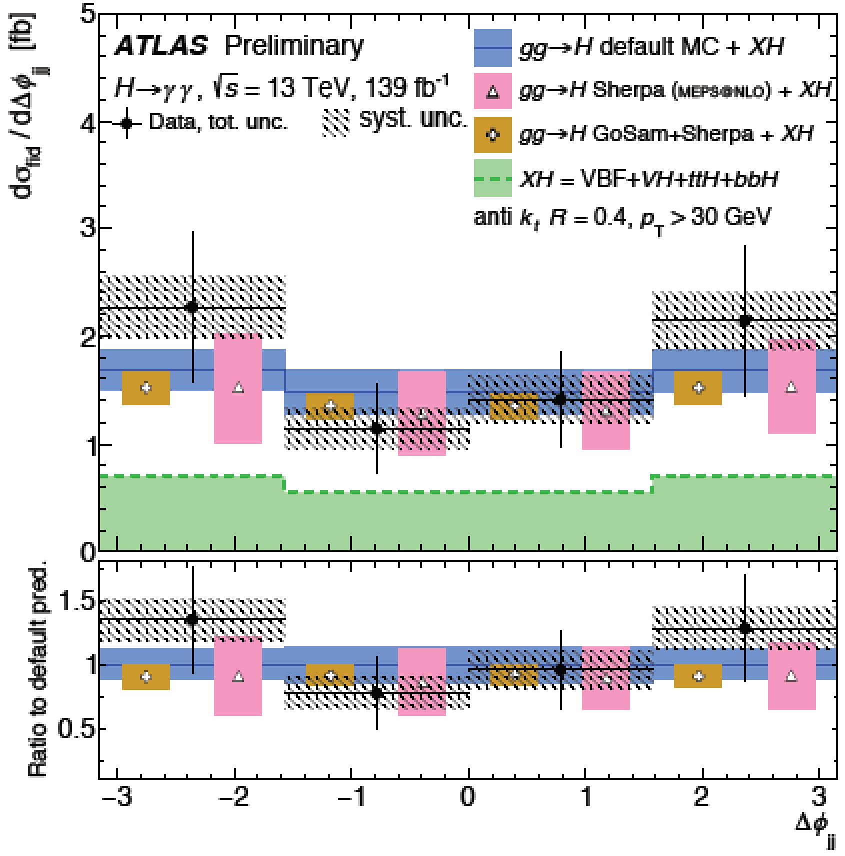

Distribution	$p(\chi^2)$ with Default MC Prediction
$p_T^{\gamma\gamma}$	44%
$\lvert y_{\gamma\gamma}\rvert$	68%
p_T^{j1}	77%
N_{jets}	96%
$\Delta\phi_{jj}$	82%
m_{jj}	75%

H→ZZ→4ℓ: m_{12} and m_{34}

m_{12} and m_{34} single fiducial differential cross section measurements in ATLAS

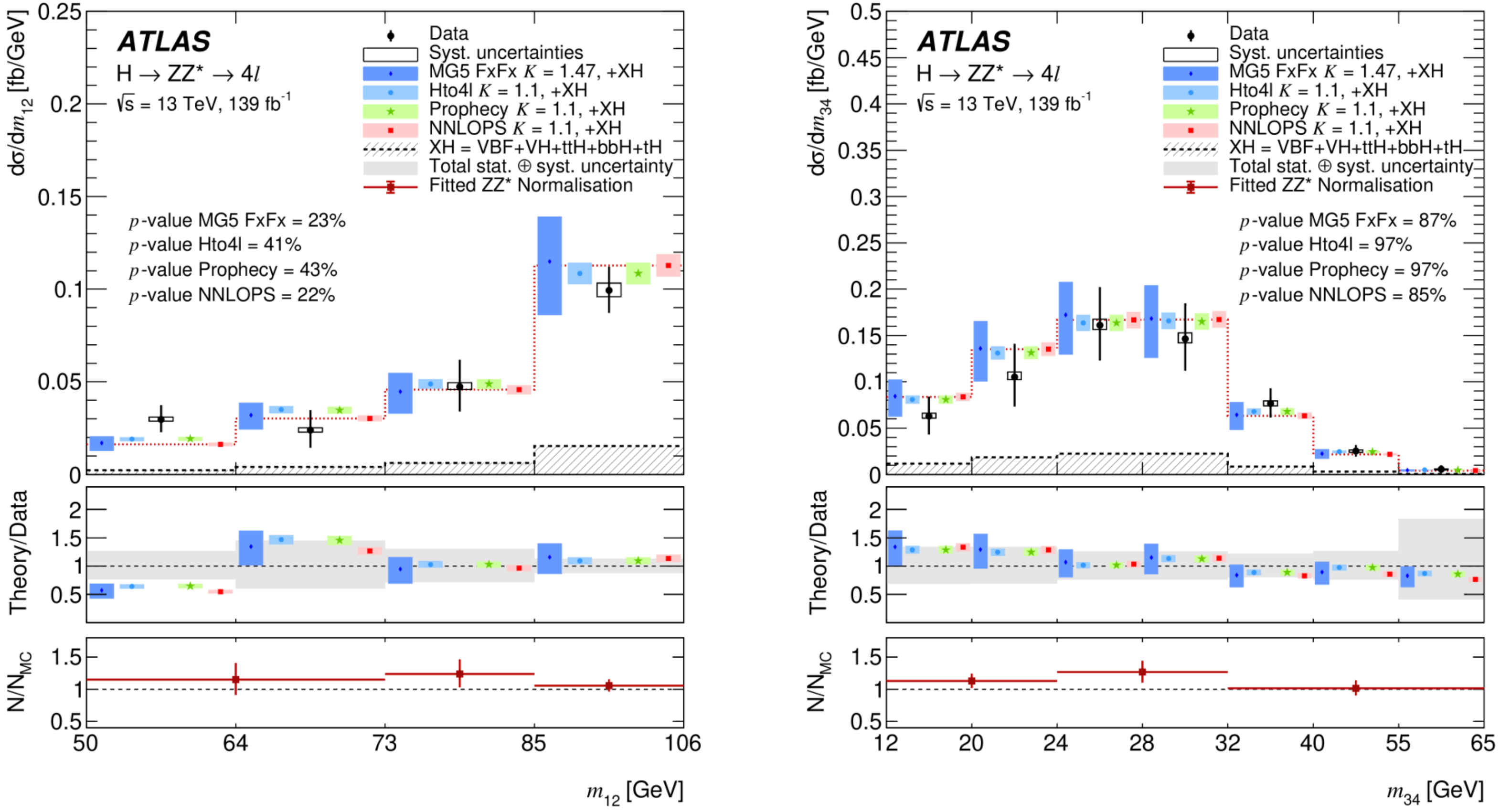

- Sensitive to higher-order electroweak corrections to the Higgs boson decay
- Sensitive to BSM contributions

H→ZZ→4ℓ : θ^*, θ_1, θ_2, ϕ, ϕ_1

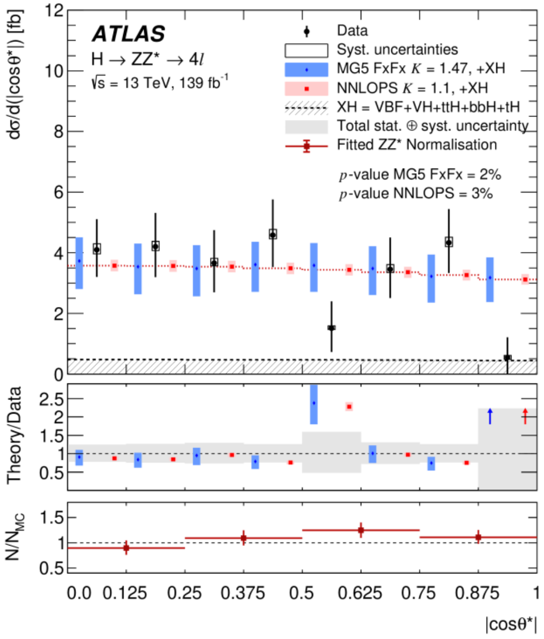

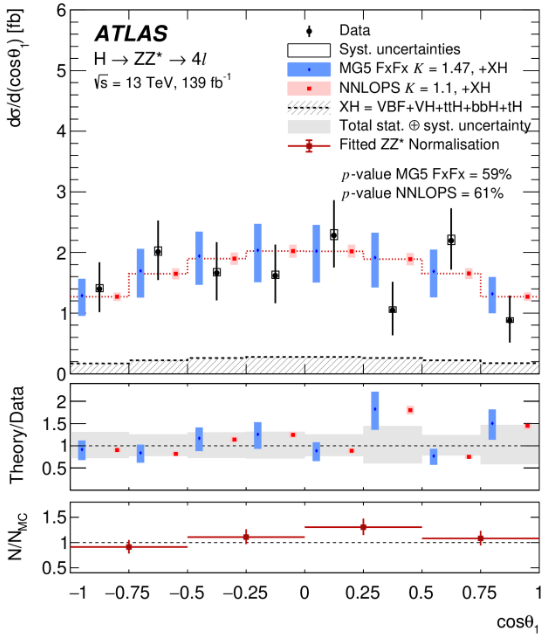

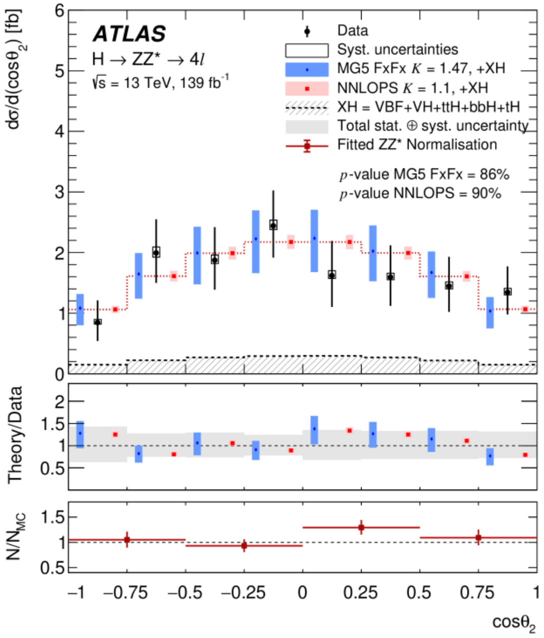

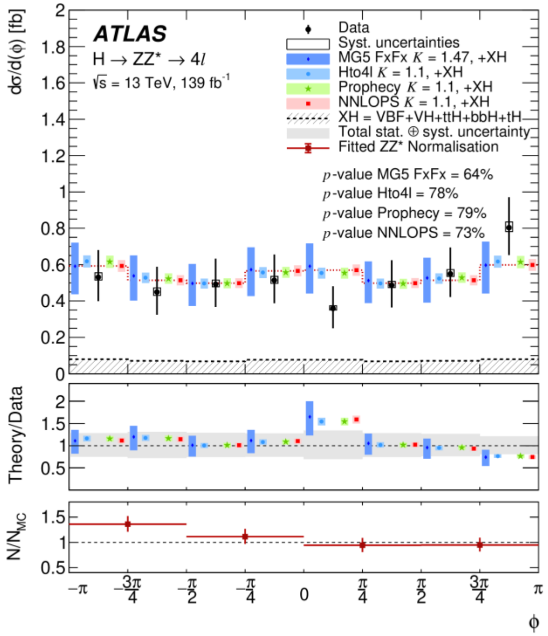

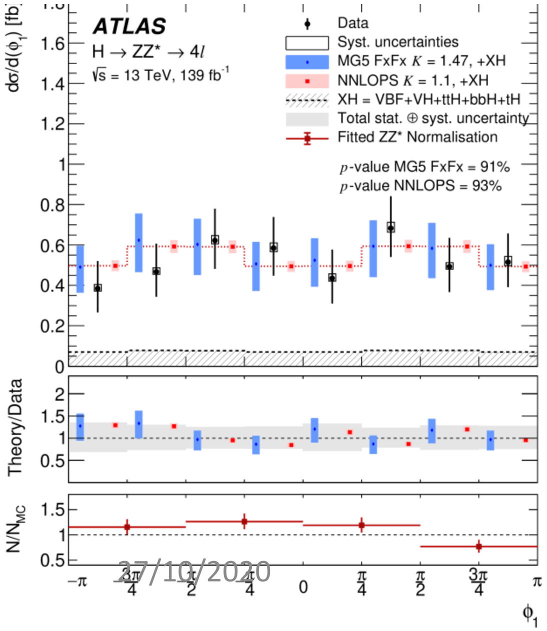

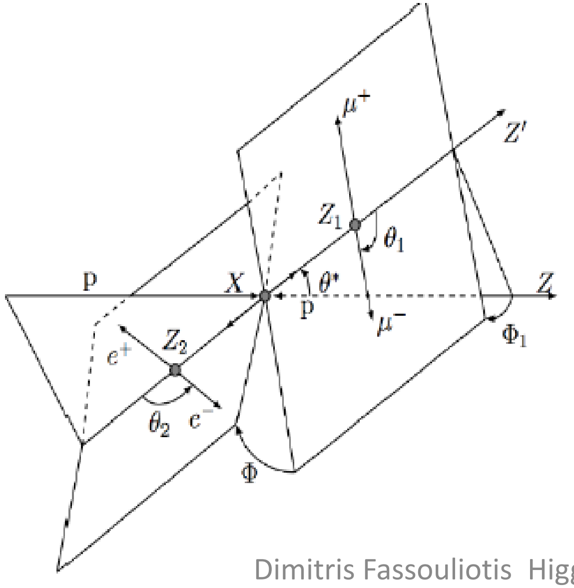

- ➢ Probe spin-CP properties
- ➢ Sensitive to the properties of the decay products

H→ZZ→4ℓ: 2d differential xs measurements

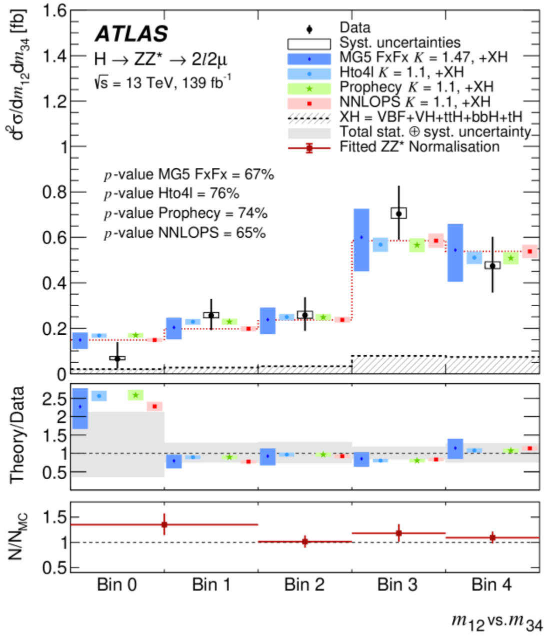

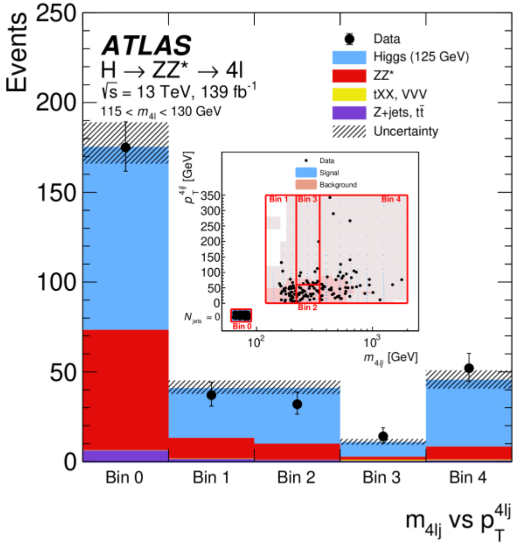

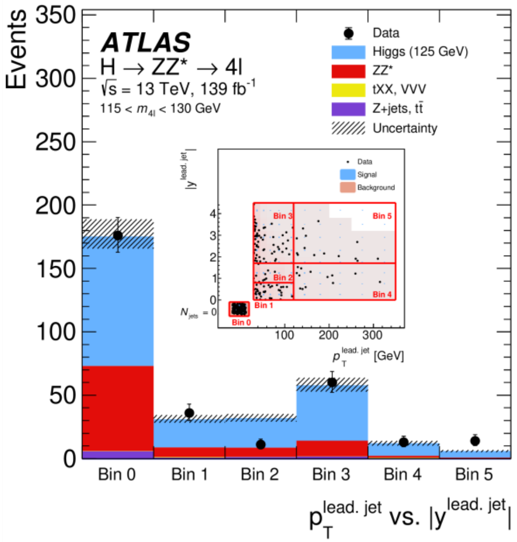

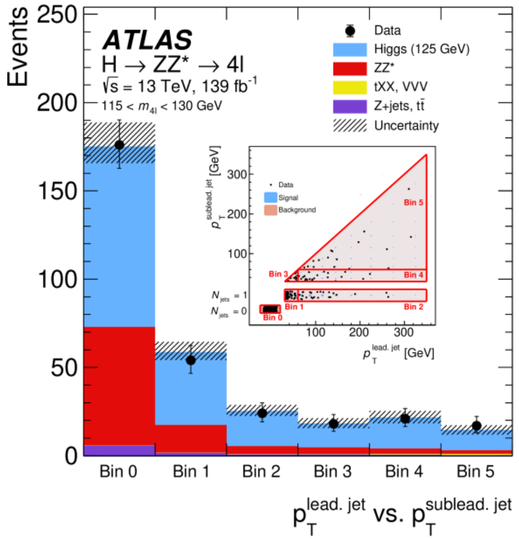

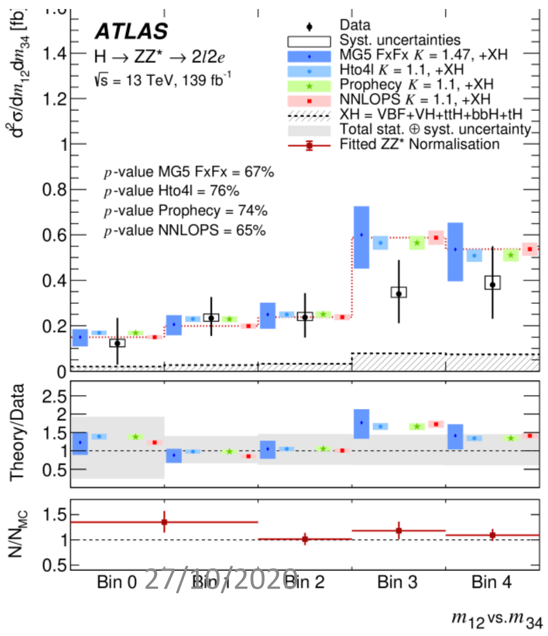

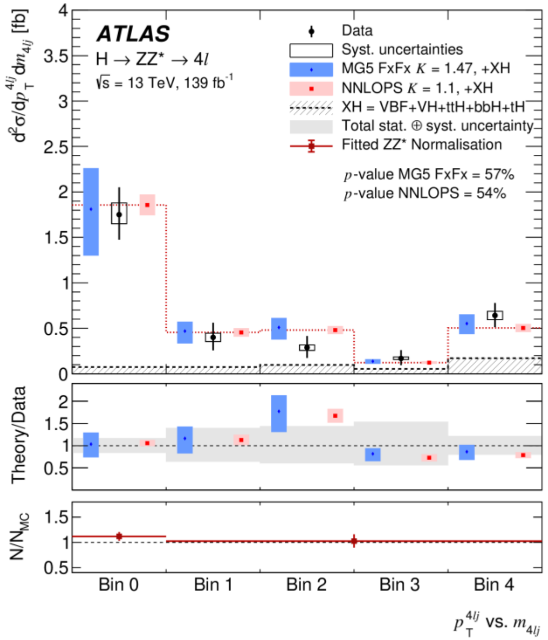

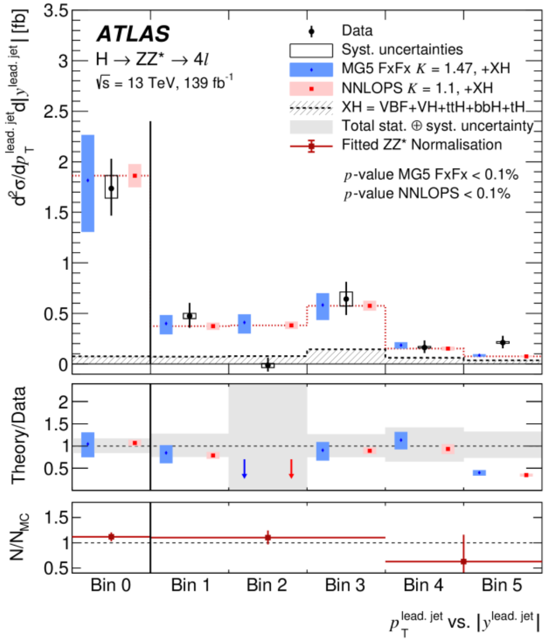

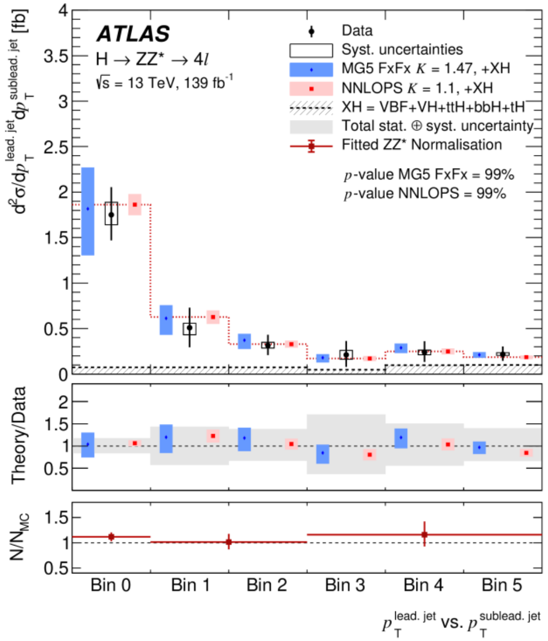

Systematic uncertainties

ATLAS $H\rightarrow ZZ\rightarrow 4\ell$

Observable	Stat. unc. [%]	Syst. unc. [%]	Dominant systematic components [%] Lumi.	e/μ	Jets	Other Bkg.	ZZ^* Th.	Sig. Th.	Comp.
σ_{comb}	9	3	1.7	2	< 0.5	< 0.5	1.0	1.5	< 0.5
$\sigma_{4\mu}$	15	4	1.7	3	< 0.5	< 0.5	1.5	1.0	< 0.5
σ_{4e}	26	8	1.7	7	< 0.5	< 0.5	1.5	1.5	< 0.5
$\sigma_{2\mu 2e}$	20	7	1.7	5	< 0.5	< 0.5	2	1.5	< 0.5
$\sigma_{2e2\mu}$	15	3	1.7	2	< 0.5	< 0.5	1	1.5	< 0.5
$d\sigma / dp_T^{4\ell}$	20–46	2–8	1.7	1–3	1–2	< 0.5	1–6	1–2	< 1
$d\sigma / dm_{12}$	12–42	3–6	1.7	2–3	< 1	< 0.5	1–2	1–2	< 1
$d\sigma / dm_{34}$	20–82	3–12	1.7	2–3	< 1	1–2	1–8	1–3	< 1
$d\sigma / d\|y_{4\ell}\|$	22–81	3–6	1.7	2–3	< 1	< 0.5	1–5	1–3	< 1
$d\sigma / d\|\cos\theta^*\|$	23–113	3–6	1.7	2–3	< 1	1–2	1–7	1–3	< 0.5
$d\sigma / d\cos\theta_1$	23–44	3–6	1.7	2–3	< 1	< 0.5	1–3	1–2	< 1
$d\sigma / d\cos\theta_2$	22–39	3–6	1.7	2–3	< 1	< 0.5	1–3	1–3	< 1
$d\sigma / d\phi$	20–29	2–5	1.7	2–3	< 1	< 0.5	1–3	1–2	< 0.5
$d\sigma / d\phi_1$	22–33	3–6	1.7	2–3	< 1	< 0.5	1–2	1–3	< 0.5
$d\sigma / dN_{jets}$	15–37	6–14	1.7	1–3	4–10	< 0.5	1–4	3–7	1–4
$d\sigma / dN_{b-jets}$	15–67	6–15	1.7	1–3	4–5	1–3	1–2	3–9	1–4
$d\sigma / dp_T^{lead.\ jet}$	15–34	3–13	1.7	1–3	4–10	< 0.5	1–2	1–5	< 0.5
$d\sigma / dp_T^{sublead.\ jet}$	11–67	5–22	1.7	1–3	2–12	< 1	1–3	2–15	1–5
$d\sigma / dm_{jj}$	11–50	5–18	1.7	1–3	1–11	< 0.5	1–3	2–15	1–2
$d\sigma / d\eta_{jj}$	11–57	5–17	1.7	1–3	2–10	< 0.5	1–2	2–14	1–4
$d\sigma / d\phi_{jj}$	11–50	4–18	1.7	1–3	2–9	< 0.5	1–3	2–14	1–6
$d\sigma / dm_{4\ell j}$	15–66	4–19	1.7	1–3	3–9	< 0.5	1–6	3–14	1–8
$d\sigma / dm_{4\ell jj}$	11–182	5–67	1.7	1–3	4–24	< 0.5	1–5	2–35	1–9
$d\sigma / dp_T^{4\ell j}$	15–76	6–13	1.7	1–3	2–8	< 1	1–5	3–9	1–3
$d\sigma / dp_T^{4\ell jj}$	11–76	5–27	1.7	2–3	2–9	1–2	1–4	3–17	1–12
$d^2\sigma / dm_{12}dm_{34}$	16–65	3–11	1.7	2–3	< 1	1–2	1–9	1–3	1–2
$d^2\sigma / dp_T^{4\ell}d\|y_{4\ell}\|$	23–63	2–13	1.7	1–3	1–2	< 1	1–6	1–5	1–2
$d^2\sigma / dp_T^{4\ell}dN_{jets}$	23–93	4–193	1.7	2–14	2–25	1–3	1–7	1–12	1–92
$d^2\sigma / dp_T^{4\ell j}dm_{4\ell j}$	15–41	4–12	1.7	1–3	2–8	< 0.5	1–5	2–9	< 1
$d^2\sigma / dp_T^{4\ell}dp_T^{4\ell j}$	15–53	3–10	1.7	1–3	2–8	< 1	1–2	2–6	1–2
$d^2\sigma / dp_T^{4\ell}dp_T^{lead.\ jet}$	15–84	3–21	1.7	1–3	2–18	1–10	1–3	2–9	1–3
$d^2\sigma / dp_T^{lead.\ jet}d\|y^{lead.\ jet}\|$	15–38	3–11	1.7	1–3	2–9	< 0.5	1–2	1–4	1–2
$d^2\sigma / dp_T^{lead.\ jet}dp_T^{sublead.\ jet}$	15–63	5–22	1.7	1–3	4–15	< 0.5	1–4	3–11	1–7

ATLAS $H\rightarrow\gamma\gamma$
Inclusive fiducial cross section

Source	Uncertainty (%)
Statistics	6.9
Signal extraction syst.	7.9
Photon energy scale & resolution	4.6
Background modelling (spurious signal)	6.4
Correction factor	2.6
Pile-up modelling	2.0
Photon identification efficiency	1.2
Photon isolation efficiency	1.1
Trigger efficiency	0.5
Theoretical modelling	0.5
Photon energy scale & resolution	0.1
Luminosity	1.7
Total	11.0